Journal of ELECTRONIC MATERIALS, Vol. 45, No. 11, 2016
DOI: 10.1007/s11664-016-4792-y

Synthesis, Surface Modification and Optical Properties of Thioglycolic Acid-Capped ZnS Quantum Dots for Starch Recognition at Ultralow Concentration

MAHNOUSH TAYEBI,[1] MOHAMMAD TAVAKKOLI YARAKI,[1,7] MAHNAZ AHMADIEH,[1] AZADEH MOGHAREI,[1] MOHAMMADREZA TAHRIRI,[2,3,4,8] DARYOOSH VASHAEE,[5] and LOBAT TAYEBI[2,6]

1.—Department of Chemical Engineering, Amirkabir University of Technology (Tehran Polytechnic), Tehran, Iran. 2.—Marquette University School of Dentistry, Milwaukee, WI 53233, USA. 3.—Dental Biomaterials Department, School of Dentistry, Tehran University of Medical Sciences, Tehran, Iran. 4.—Biomaterials Group, Faculty of Biomedical Engineering, Amirkabir University of Technology (Tehran Polytechnic), Tehran, Iran. 5.—Electrical and Computer Engineering Department, North Carolina State University, Raleigh, NC 27606, USA. 6.—Department of Engineering Science, University of Oxford, Oxford OX1 3PJ, UK. 7.—e-mail: mty206@aut.ac.ir. 8.—e-mail: mohammadreza.tahriri@marquette.edu

In this research, water-soluble thioglycolic acid-capped ZnS quantum dots (QDs) are synthesized by the chemical precipitation method. The prepared QDs are characterized using x-ray diffraction and transmission electron microscopy. Results revealed that ZnS QDs have a 2.73 nm crystallite size, cubic zinc blende structure, and spherical morphology with a diameter less than 10 nm. Photoluminescence (PL) spectroscopy is performed to determine the presence of low concentrations of starch. Four emission peaks are observed at 348 nm, 387 nm, 422 nm, and 486 nm and their intensities are quenched by increasing concentration of starch. PL intensity variations in the studied concentrations range (0–100 ppm) are best described by a Michaelis–Menten model. The Michaelis constant (K_m) for immobilized α-amylase in this system is about 101.07 ppm. This implies a great tendency for the enzyme to hydrolyze the starch as substrate. Finally, the limit of detection is found to be about 6.64 ppm.

Key words: ZnS QDs, starch, α-amylase, thioglycolic acid, photoluminescence, concentration

INTRODUCTION

Starch, a polysaccharide, consists of glucose units, with alpha-1,4 and alpha-1,6 glycosidic bonds and has been used in water treatment industries as a coagulant.[1] Starch is used in the form of anionic, cationic, and non-ionic starch-based materials to increase the efficiency of water treatment processes.[2] Starch derivative compounds, originating from either their use as coagulant in water treatment processes or raw water sources may remain in treated potable water and cause an undesirable growth of bacteria in water distribution systems.[3]

Various methods are used to measure starch directly and quantitatively including calorimetry,[4] high performance liquid chromatography (HPLC),[5] immobilized enzymes,[6] multi-enzymes electrodes,[7] and formation of colored complexes (e.g., interaction of iodine with starch).[8] However, these methods are complicated, expensive, and time-consuming. Two of the most reliable and reproducible methods are McCleary et al.'s method[9] and Ewers' polarimetric method,[10] now widely accepted by the American Association of Cereal Chemists (AACC) and the European Community (EC), respectively.

Nanotechnology is empowering technology that deals with nanometer-sized objects. It is expected

Mahnoush Tayebi and Mohammad Tavakkoli Yaraki contributed equally to this work.
(Received May 16, 2016; accepted July 7, 2016; published online August 5, 2016)

that nanotechnology will be created at different levels: materials, devices, and systems.[11–45] Quantum dots (QDs) are semiconductor nanocrystals with a diameter of 2 nm–100 nm. They are commonly used as high-sensitive optical sensors due to their unique luminescence properties such as narrow emission bandwidth, size-dependent tunable photoluminescence, longer fluorescence lifetime, and high brightness as a result of quantum confinement.[46–56] ZnS is one of the first QDs to be discovered and is applied for sensors and biodevices because of its large band gap of ~3.77 eV and ~3.72 eV for hexagonal wurtzite (WZ) and cubic zinc blende (ZB) ZnS, respectively.[57]

The aim of this evaluation is to develop a reliable, rapid, inexpensive, and sensitive fluorescent-based biosensor for determination of low concentrations of starch remained in drinking water. Starch quantification is based on photoluminescence variations of colloidal ZnS QDs linked to starch enzyme called alpha-amylase enzyme.[58]

EXPERIMENTAL PROCEDURE

Reagents

Soluble starch, glucose, zinc acetate dehydrate, sodium sulfide, thioglycolic acid (TGA), and sodium hydroxide were purchased from Merck, Germany. *Bacillus*-derived alpha-amylase enzyme was purchased from SERVA, Germany. All chemicals were in analytical grade.

Synthesis of Surface Modified TGA-Capped ZnS Quantum Dots

The ZnS colloidal QDs solution is synthesized using a reaction between Zn^{2+} and S^{2-} ions at ambient temperature and in the presence of TGA as the stabilizer and size-controlling agent. Our method is similar to that used by Xiao et al.[59] with minor modifications. Firstly, 20 mL of a 0.05 M zinc acetate solution is obtained by dissolving the required amount of zinc acetate dihydrate in double distilled water. Then, 0.25 ml of TGA is added to the above mixture at 80°C and vigorously stirred for 30 min. Afterwards, 20 ml Na_2S stock solution is added dropwise to the above mixture and then stirred continuously for 2 h. A change in opacity of the solution is an indication of ZnS formation in the reaction vessel. The resulted colloidal solution is used for further tests.

As acidic conditions destroy the QDs[60] and α-amylase is not active in acidic pH, colloidal TGA-capped ZnS QDs are neutralized by adding the required amount of 1 M NaOH. Then, 5 ml of a 500 ppm α-amylase solution is added to the reaction vessel and stirred vigorously at ambient temperature for 30 min.

Preparation of Sample Solutions

First, standard starch solutions are prepared by adding the required amount of starch to double distilled water. Then, 1 ml of each sample is added to 15 ml of the colloidal solution of α-amylase immobilized on ZnS QDs at pH 7 and 40°C under vigorous stirring for 30 min. Finally, photoluminescence spectra of each reaction vessel is measured by exciting at 264 nm.

Apparatus

Transmission electron microscopy (TEM) micrographs are recorded by a Hitachi H-800 and x-ray measurements are performed using an Equinox 3000 diffractometer utilizing radiation Cu-K_α

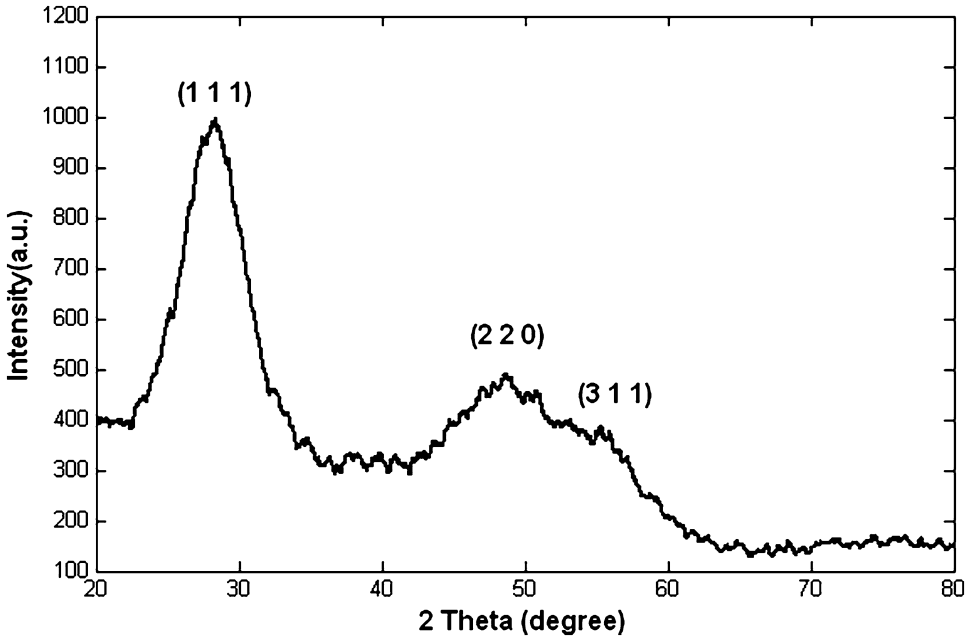

Fig. 1. XRD patterns for the synthesized TGA-capped ZnS QDs.

(λ = 1.5406 Å). The fluorescence spectra and intensities are measured with a Perkin-Elmer LS55 spectrophotometer for which the slit width is set at 5 nm for both excitation and emission. All optical measurements are performed at room temperature.

RESULTS AND DISCUSSION

Characterization of TGA-Capped ZnS Quantum Dots

Colloidal solution of ZnS QDs are centrifuged at 5000 rpm and then washed two times with ethanol for x-ray diffraction (XRD) analysis. Figure 1 reveals the XRD patterns for ZnS QDs. As it can be seen in Fig. 1, there are three peaks at about 2θ = 27°, 48°, and 57°. This means that our synthesized ZnS QDs can be indexed as cubic zinc blende phase structure (JCPDS 5-566). The crystallite size can be calculated from Debye–Schrerr equation defined as below[59]:

$$D = \frac{0.9\lambda}{\text{FWHM}\cos(\theta)}, \quad (1)$$

where D, θ, λ, and FWHM are crystallite size, degree of maximum peak in XRD patterns, x-ray wavelength, and full width at half maximum in the XRD patterns, respectively. The crystallite size of ZnS QDs is calculated to be about 2.73 nm.

For the TEM micrograph, the colloidal ZnS QDs solution is used. Figure 2 shows TGA-capped ZnS QDs. As it can be observed in this figure, the particles have a size of less than 10 nm and spherical morphology.

Figure 3 shows emission spectra of our colloidal ZnS QDs. There are four peaks at λ = 348 nm, 387 nm, 422 nm, and 486 nm. In colloidal ZnS, vacancy states lie deeper in the gap than states arising from interstitial atoms.[61] Therefore, we conclude that the two short wavelength peaks at 348 nm and 387 nm, and the two long ones at 422 nm and 486 nm are due to transitions involving interstitial states and vacancy states, respectively. Denzler et al.[62] have also reported four peaks for colloidal ZnS QDs synthesized by the chemical precipitation method. Based on their results and discussion, interstitial sulfur states and sulfur vacancy states should be located closer to the valence band edge than interstitial zinc states and

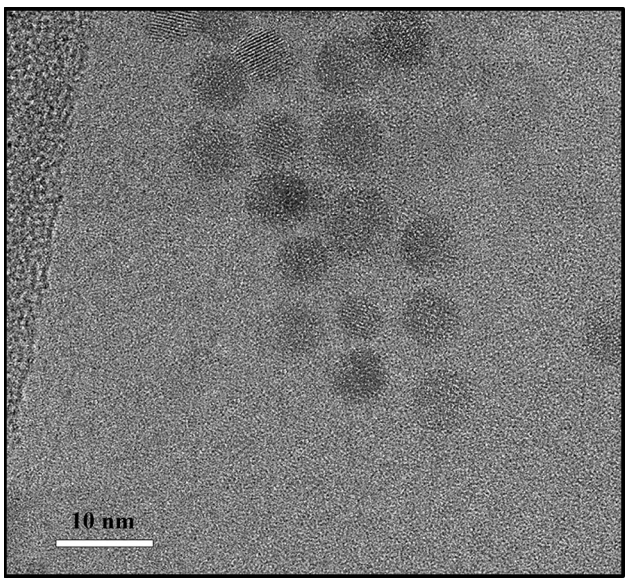

Fig. 2. TEM micrograph of the TGA-capped ZnS QDs.

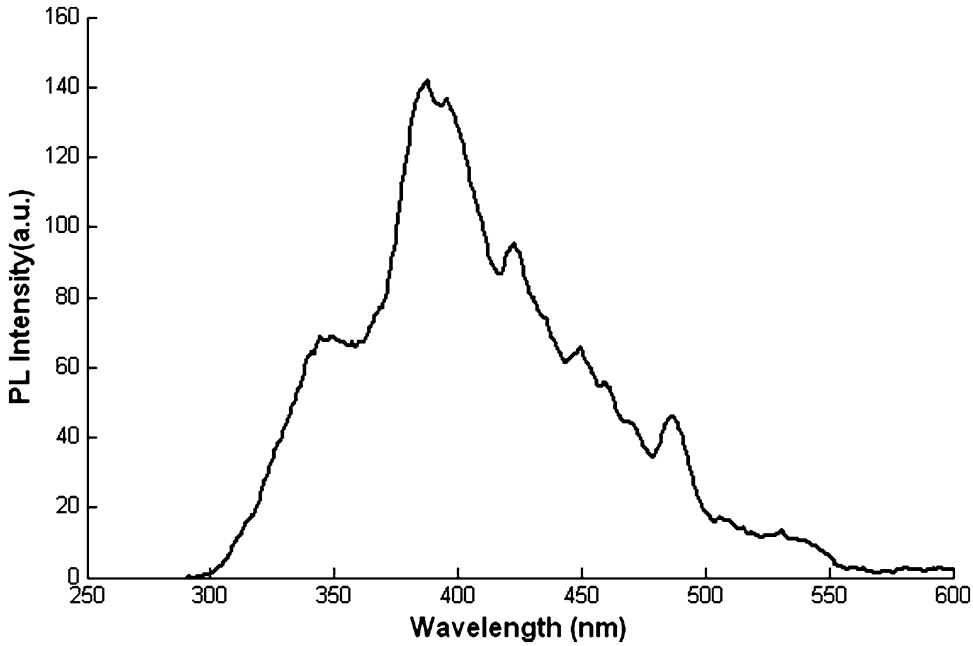

Fig. 3. Photoluminescence emission spectra of colloidal ZnS QDs, excited at 264 nm.

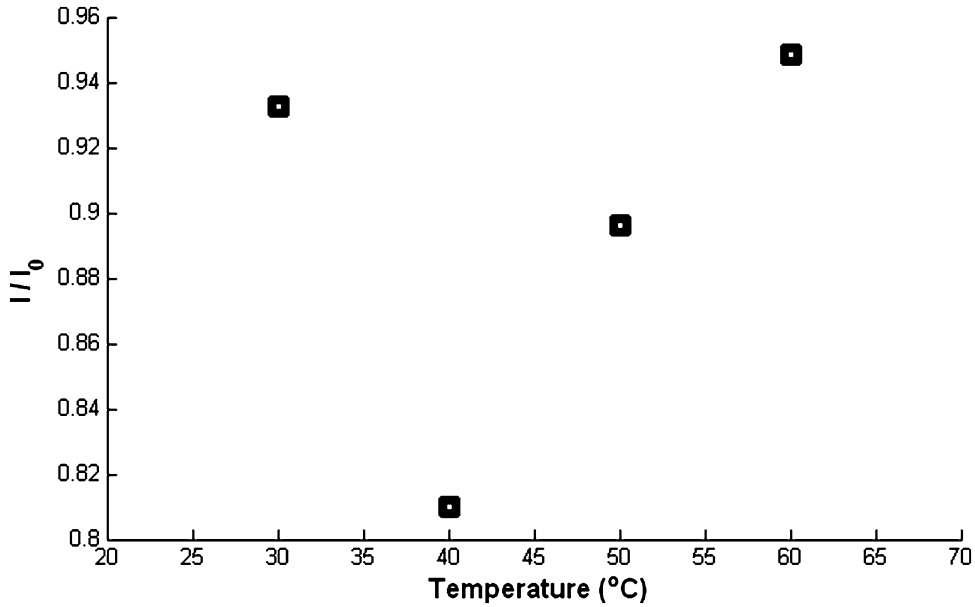

Fig. 4. Effect of temperature of the starch hydrolysis reaction on PL intensities of enzyme-capped ZnS QDs at pH = 7.

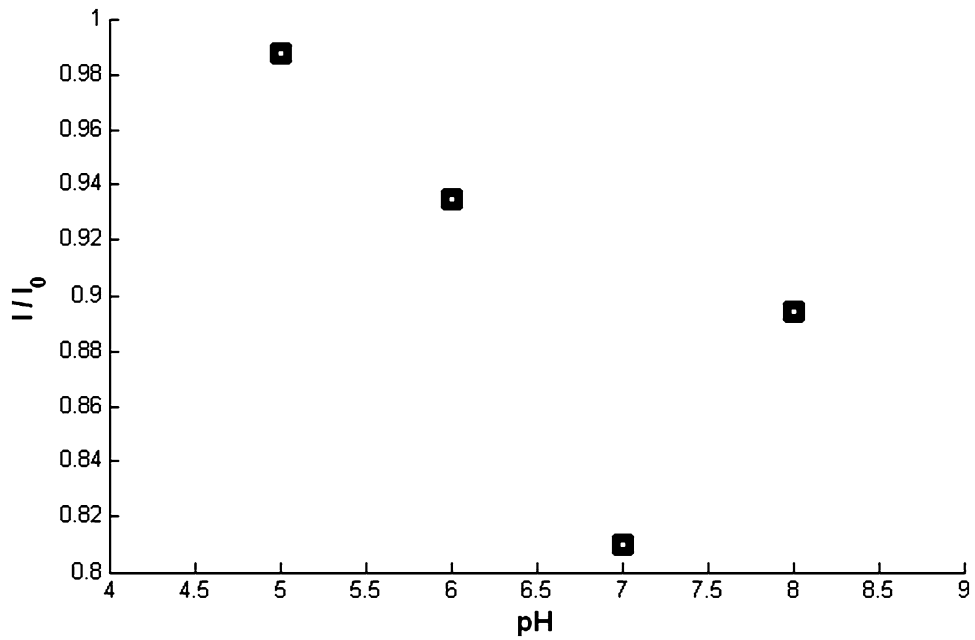

Fig. 5. Effect of pH of the starch hydrolysis reaction on PL intensities of enzyme-capped ZnS QDs at 40°C.

zinc vacancy states to the conduction band edge. Consequently, we attribute the peak at 348 nm and 387 nm to the sulfur and zinc vacancy, respectively, and the ones at 422 nm and 487 nm to interstitial sulfur and zinc, respectively.

Photoluminescence (PL) emission of ZnS QDs is strongly depended on surface modification, synthesis method, and conditions.[63] In most cases, only one[64,65] or two[66,67] and sometimes four[62] peaks are reported for fluorescence emissions of ZnS QDs.

Conjugating α-Amylase to ZnS QDs and Its Activity

To determine the optimum conditions (pH and temperature) for enzyme activity, we carried out additional experiments. As optimum conditions for activity of α-amylase are reported to be 40°C and pH = 7,[68,69] we assumed that these conditions were also optimal for α-amylase immobilized on ZnS QDs. We used these conditions as a starting point to find

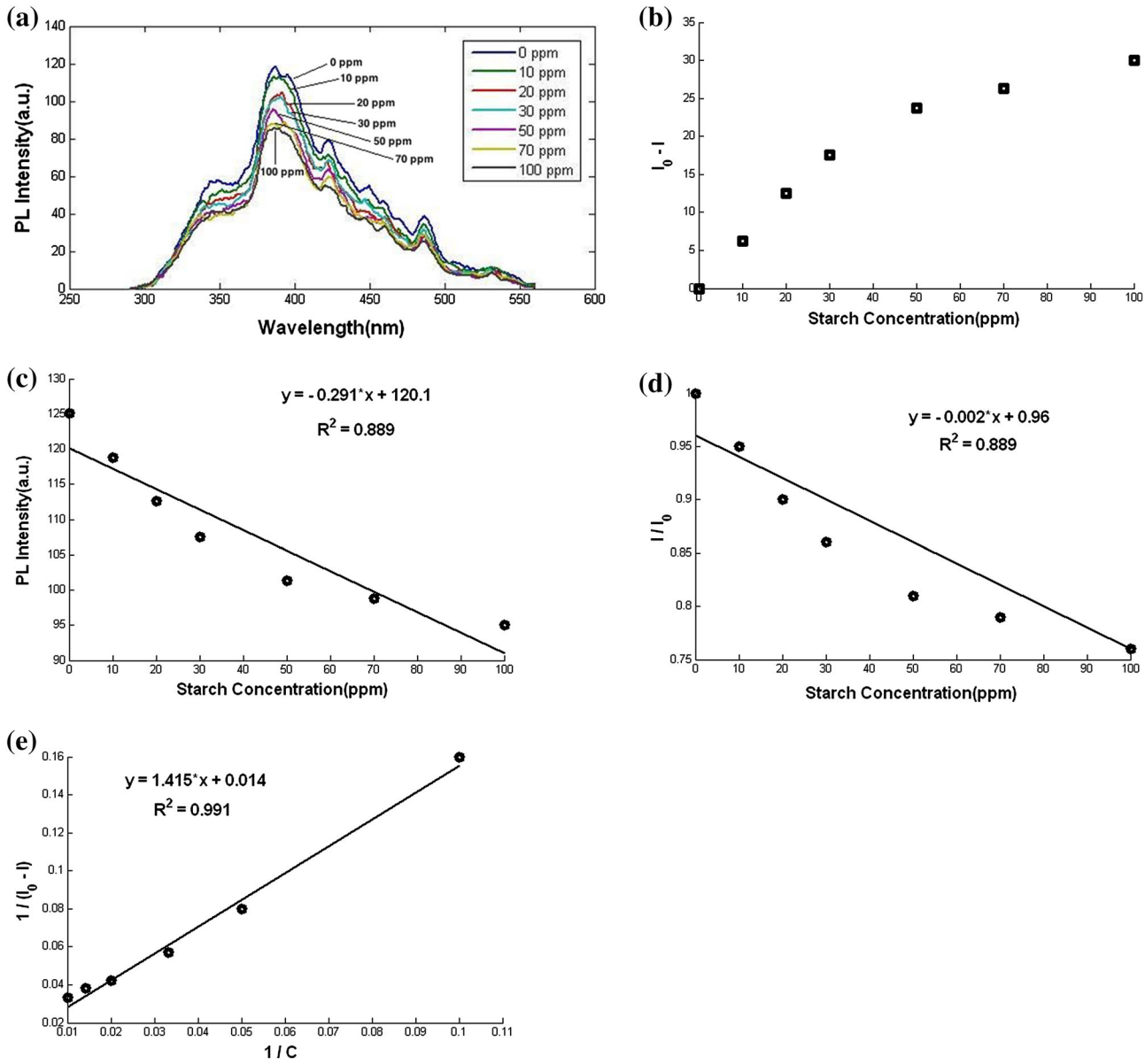

Fig. 6. (a) Photoluminescence study of enzyme-capped ZnS QDs in the presence of standard starch solutions with different concentrations, (b) Comparative PL intensity variations with starch concentration, (c) PL intensity as a function of starch concentration (d) changes of relative PL intensity with starch concentration and (e) The Linwearer-Bruke plot for the Michaelis–Menten model based on the results presented in the current work.

Table I. Reported K_m for α-amylase from different sources

Enzyme source	K_m (ppm)	Reference
Bacillus licheniformis	8300	73
β-amyloliquefaciens	4110	74
Lactobacillusmanihotivor	2440	75
Bacillus	101.07	Current work

the optimum enzyme activity conditions for our QDs. We spanned the temperature-pH space once by keeping the pH constant at 7 and changing the temperature and once by maintaining a temperature of 40°C and varying the pH. We added 1 ml of a 50 ppm starch solution in doubled distilled water to the above reaction vessel at various conditions and performed PL measurements. According to Figs. 4 and 5, the largest PL intensity quench was observed at pH = 7 and 40°C, the starting point condition.

Photoluminescence Study

Figure 6a reveals the PL intensity of each reaction vessel. PL intensity quenches by increasing starch concentration. In Fig. 6b, comparative PL intensity (I_0–I) also increased by increasing starch

Table II. Effect of glucose as an impurity on the relative error between the starch concentrations calculated from the M–M model and the actual concentration in each sample

Glucose (ppm)	Starch (ppm)	Starch from M–M model (ppm)	Relative error (%)
10	90	90.21	0.23
30	70	70.37	0.53
50	50	49.53	−0.94

concentration, and it did not remain constant for high concentrations samples, therefore, we concluded that this system could be used for starch determination with concentration much higher than 100 ppm.[70] As the aim of this project is the determination of starch at low concentration, it is not relevant to find the high limit of quantification for this system. Figure 6c indicates that with an increase in starch concentration, PL intensity decreased non-linearly for all samples. Figure 6d shows changes of relative PL intensity (I/I_0) with starch concentration. This figure confirms our conclusion from Fig. 6b because relative PL intensity for 100 ppm starch is just about 0.76, which shows that the capacity of this system is higher than 100 ppm.

Michaelis–Menten Model

The Michaelis–Menten model (M–M) is a model used for investigation of immobilized enzyme affinity to the substrate.[71] M–M model is defined by the following equation:

$$\frac{1}{I_0 - I} = \frac{K_m}{V_{max}}\frac{1}{C} + \frac{1}{V_{max}}, \qquad (2)$$

where I_0–I is the comparative PL intensity, C is the starch concentration in ppm, and K_m and V_{max} are constants. Small values of the Michaelis constant (K_m) indicate the high affinity of enzyme for the substrate.[72] Figure 6e presents the Linweaver-Bruke plot for M–M model based on PL intensity results in this work. PL data agree very well with the M–M model and this model can be used as a standard curve for low concentration starch determination. Table I shows the value of K_m in different studies for α-amylase with starch as substrate. K_m for this system is considerably lower than other reported values, which indicates that α-amylase immobilized on ZnS QDs has a high tendency to hydrolyze starch as substrate.

Limit of Detection (LOD)

As PL intensity changes linearly with starch concentration (see Fig. 6c), the limit of detection can be determined using the equation LOD $= \frac{3\sigma}{s}$, (where σ is the standard deviation of blank measurements of six replicates containing 10 ppm starch and S is the absolute value of slope obtained from Fig. 6c). For our ZnS QDs, the limit of detection for starch is calculated to be 6.64 ppm.

Selectivity

Selectivity and the effect of impurities is studied by using three mixtures of starch and glucose with varying ratios of starch to glucose and a total concentration of 100 ppm. As shown in Table II, there is a less than 1 % relative error between the starch concentrations calculated from the M–M model and the actual concentration in each sample. Therefore, our designed fluorescence-based sensor is very selective in determination of starch.

CONCLUSIONS

In conclusion, colloidal TGA-capped ZnS QDs are successfully synthesized using the chemical precipitation method. α-amylase is used as a starch-converting enzyme and is immobilized on colloidal ZnS QDs. A linear quench in PL intensity is observed with an increase in starch concentration. Our data is best described by the Michaelis–Menten model. The ultralow Michaelis constant (K_m) indicates the high affinity of immobilized enzyme to starch as substrate. This fluorescence-based detection method is reliable, rapid, inexpensive, and very sensitive. Eventually, PL data agree very well with the M–M model, and this model can be employed as a standard curve for determination of starch concentrations less than 100 ppm in different samples.

ACKNOWLEDGEMENT

The authors would like to acknowledge Prof. F. Vahabzadeh for her help in this project.

REFERENCES

1. A. Ye, Y. Hemar, and H. Singh, *Colloids Surf. B* 38, 1 (2004).
2. G. Xing, S. Zhang, B. Ju, and J. Yang, eds., in *Proceedings of the Third International Conference on Functional Molecules* (2005).
3. D. Van der Kooij and W. Hijnen, *Appl. Environ. Microbiol.* 49, 765 (1985).
4. M. Séne, C. Thévenot, and J. Prioul, *J. Cereal Sci.* 26, 211 (1997).
5. N. Boley and M. Burn, *Food Chem.* 36, 45 (1990).
6. L.H. Lim, D.G. Macdonald, and G.A. Hill, *Biochem. Eng. J.* 13, 53 (2003).
7. T. Hu, X.-E. Zhang, and Z.-P. Zhang, *Biotechnol. Tech.* 13, 359 (1999).

8. N. Sakač, M. Sak-Bosnar, and M. Horvat, *Food Chem.* 138, 9 (2013).
9. B. McCleary, V. Solah, and T. Gibson, *J. Cereal Sci.* 20, 51 (1994).
10. G.A. Mitchell, *Starch-Stärke* 42, 131 (1990).
11. M. Tahriri, M. Solati-Hashjin, and H. Eslami, *Iranian J. Pharm. Sci.* 4, 127 (2008).
12. E. Shafia, M. Bodaghi, and M. Tahriri, *Curr. Appl. Phys.* 10, 596 (2010).
13. M. Mozafari, F. Moztarzadeh, M. Rabiee, M. Azami, N. Nezafati, Z. Moztarzadeh, and M. Tahriri, *Adv. Compos. Lett.* 19, 91 (2010).
14. M. Bodaghi, A. Mirhabibi, H. Zolfonun, M. Tahriri, and M. Karimi, *Phase Transit.* 81, 571 (2008).
15. F. Kazemi, A. Saberi, S. Malek-Ahmadi, S. Sohrabi, H. Rezaie, and M. Tahriri, *Ceramics-Silikáty* 55, 26 (2011).
16. H. Eslami, M. Solati-Hashjin, and M. Tahriri, *Adv. Appl. Ceram. Struct. Funct. Bioceram.* 109, 200 (2010).
17. H. Eslami, M. Tahriri, and F. Bakhshi, *Mater. Sci. Pol.* 28, 5 (2010).
18. H. Sameie, R. Salimi, A.S. Alvani, A. Sarabi, F. Moztarzadeh, and M. Tahriri, *Phys. B Condens. Matter* 405, 4796 (2010).
19. M. Bodaghi, A. Mirhabibi, M. Tahriri, H. Zolfonoon, and M. Karimi, *Mater. Sci. Eng. B.* 162, 155 (2009).
20. M. Bodaghi, H. Zolfonoon, M. Tahriri, and M. Karimi, *Solid State Sci.* 11, 496 (2009).
21. M. Tahriri and F. Moztarzadeh, *Appl. Biochem. Biotechnol.* 172, 2465 (2014).
22. M.E. Khosroshahi, L. Ghazanfari, and M. Tahriri, *J. Exp. Nanosci.* 6, 580 (2011).
23. R. Salimi, H. Sameie, A.S. Alvani, A. Sarabi, H.E. Mohammadloo, F. Nargesian, M. Sabbagh Alvani, and M. Tahriri, *JOSA B* 30, 1747 (2013).
24. R. Salimi, H. Sameie, A.S. Alvani, A. Sarabi, F. Moztarzadeh, H.E. Mohammadloo, F. Nargesian, and M. Tahriri, *J. Mater. Sci.* 47, 2658 (2012).
25. R. Salimi, H. Sameie, A. Sabbagh Alvani, A. Sarabi, F. Moztarzadeh, and M. Tahriri, *Luminescence* 26, 449 (2011).
26. E. Shafia, A. Aghaei, A. Davarpanah, M. Bodaghi, M. Tahriri, and S. Alavi, *Trans. Indian Ceram. Soc.* 70, 71 (2011).
27. K. Khoshroo, T.S. Jafarzadeh Kashi, F. Moztarzadeh, H. Eslami, and M. Tahriri, *Synth. React. Inorganic Metal Organic Nano Metal Chem.* 46, 1189 (2016).
28. F.M.H. Eslami, T.S.J. Kashi, K. Khoshroo, and M. Tahriri, *Synth. React. Inorganic Metal Organic Nano Metal Chem.* 46, 1149 (2016).
29. R. Masaeli, T.J. Kashi, R. Dinarvand, H.V. Rakhshan, B. Hooshmand, F.M. Abbas, et al., *Mater. Sci. Eng. C* 69, 171 (2016).
30. M. Abdorahim, M. Rabiee, S. Naghavi Alhosseini, M. Tahriri, S. Yazdanpanah, S. H. Alavi, and L. Tayebi, *TrAC Trends Anal. Chem.* 82, 337 (2016).
31. H. Eslami, F. Moztarzadeh, T. Jafarzadeh Kashi, M. Solati-Hashjin, K. Khoshroo, and M. Tahriri, *Key Eng. Mater.* 631, 198 (2015).
32. S. Solgi, M. Khakbiz, M. Shahrezaee, A. Zamanian, M. Tahriri, S. Keshtkari, M. Raz, K. Khoshroo, S. Moghadas, and A. Rajabnejad, *Silicon* (2015). doi:10.1007/s12633-015-9291-x.
33. F.S. Jazi, N. Parvin, M. Tahriri, M. Alizadeh, S. Abedini, and M. Alizadeh, *Synth. React. Inorganic Metal Organic Nano Metal Chem.* 44, 759 (2014).
34. Y. Rezaei, F. Moztarzadeh, S. Shahabi, and M. Tahriri, *Synth. React. Inorganic Metal Organic Nano Metal Chem.* 44, 692 (2014).
35. R. Touri, F. Moztarzadeh, Z. Sadeghian, D. Bizari, M. Tahriri, and M. Mozafari, *BioMed Res. Int.* 2013, 465086 (2013).
36. M. Ashuri, F. Moztarzadeh, N. Nezafati, A.A. Hamedani, and M. Tahriri, *Mater. Sci. Eng. C* 32, 2330 (2012).
37. F.S. Jazi, N. Parvin, M. Rabiei, M. Tahriri, Z.M. Shabestari, and A.R. Azadmehr, *J. Ceram. Process. Res.* 13, 523 (2012).
38. F. Shafiei, M. Behroozibakhsh, F. Moztarzadeh, M. Haghbin-Nazarpak, and M. Tahriri, *IET Micro Nano Lett.* 7, 109 (2012).
39. M. Raz, F. Moztarzadeh, A.A. Hamedani, M. Ashuri, and M. Tahriri, eds. *Key Eng. Mater.* 493, 746 (2012).
40. H. Eslami, F. Moztarzadeh, and M. Tahriri, *Mater. Res. Innov.* 15, 190 (2011).
41. M. Raz, F. Moztarzadeh, A.A. Hamedani, M. Ashuri, and M. Tahriri, *Key Eng. Mater.* 1463, 746 (2011).
42. A. Zamanian, F. Moztarzadeh, S. Kordestani, S. Hesaraki, and M. Tahriri, *Adv. Appl. Ceram.* 109, 440 (2010).
43. M. Bodaghi, A. Mirhabibi, and M. Tahriri, *Powder Metall. Metal Ceram.* 48, 634 (2009).
44. H. Sameie, R. Salimi, A.S. Alvani, A. Sarabi, F. Moztarzadeh, M.M. Farsi, H. Eivaz Mohammadloo, M. Sabbagh Alvani, and M. Tahriri, *J. Inorganic Organometall. Polym. Mater.* 22, 737 (2012).
45. B. Bahmani, F. Moztarzadeh, M. Rabiee, and M. Tahriri, *Synth. Metals* 160, 2653 (2010).
46. M. Tayebi, M. Tavakkoli Yaraki, A. Mogharei, M. Ahmadieh, D. Vashaee, and L. Tayebi, *J. Fluoresc.* (2016). doi: 10.1007/s10895-016-1870-8.
47. E. Mohagheghpour, M. Rabiee, F. Moztarzadeh, M. Tahriri, M. Jafarbeglou, D. Bizari, and H. Eslami, *Mater. Sci. Eng. C* 29, 1842 (2009).
48. M. Karimi, M. Rabiee, F. Moztarzadeh, M. Bodaghi, and M. Tahriri, *Solid State Commun.* 149, 1765 (2009).
49. M. Mozafari, F. Moztarzadeh, and M. Tahriri, *Adv. Appl. Ceram.* 110, 30 (2011).
50. E. Mohagheghpour, F. Moztarzadeh, M. Rabiee, M. Tahriri, M. Ashuri, H. Sameie, R. Salimi, and S. Moghadas, *IEEE Trans. NanoBiosci.* 11, 317 (2012).
51. E. Mohagheghpour, M. Rabiee, F. Moztarzadeh, and M. Tahriri, *J. Ceram. Process. Res.* 11, 144 (2010).
52. M. Abdolrahim, M. Rabiee, S.N. Alhosseini, M. Tahriri, S. Yazdanpanah, and L. Tayebi, *Anal. Biochem.* 485, 1 (2015).
53. M.K.S. Funkcionaliziranih, *Mater. Technol.* 47, 235 (2013).
54. E. Mohagheghpour, R. Salimi, H. Sameie, F. Moztarzadeh, M. Roohnikan, M.A. Mokhtari Farsi, Y. Ebrahimi, H. Eivaz Mohammadloo, and M. Tahriri, A new optical bio-sensor: Wet-chemical synthesis and surface treatment of nanocrystalline Zn 1-xS: Mn+2 x, in *Advanced Photonics*, OSA Technical Digest (CD) (Toronto Canada: Optical Society of America, 12–15 June, 2011), paper SWC4. doi:10.1364/SENSORS.2011.SWC4.
55. E. Mohagheghpour, F. Moztarzadeh, M. Rabiee, M. Tahriri, M. Ashuri, H. Sameie, R. Salimi, and S. Moghadas, *IEEE Trans. Nanobioscience* 11, 317 (2012).
56. M. Tayebi, M.T. Yaraki, M. Ahmadieh, M. Tahriri, D. Vashaee, and L. Tayebi, *Colloid Polym. Sci.* (2016). doi: 10.1007/s00396-016-3903-x.
57. X. Fang, T. Zhai, U.K. Gautam, L. Li, L. Wu, Y. Bando, and D. Golberg, *Progr. Mater. Sci.* 56, 175 (2011).
58. M.J. Van Der Maarel, B. Van Der Veen, J.C. Uitdehaag, H. Leemhuis, and L. Dijkhuizen, *J. Biotechnol.* 94, 137 (2002).
59. Q. Xiao and C. Xiao, *Appl. Surf. Sci.* 254, 6432 (2008).
60. M. Hardzei and M. Artemyev, *J. Luminesc.* 132, 425 (2012).
61. W.G. Becker and A.J. Bard, *J. Phys. Chem.* 87, 4888 (1983).
62. D. Denzler, M. Olschewski, and K. Sattler, *J. Appl. Phys.* 84, 2841 (1998).
63. H. Tang, G. Xu, L. Weng, L. Pan, and L. Wang, *Acta Material.* 52, 1489 (2004).
64. S. Wageh, Z.S. Ling, and X. Xu-Rong, *J. Cryst. Growth* 255, 332 (2003).
65. T. Shcherba, K. Lupandina, M. Zhilenko, G. Muravieva, H. Ehrlich, and G. Lisichkin, *Russian Chem. Bull.* 60, 1571 (2011).
66. M.J. Iqbal and S. Iqbal, *J. Luminesc.* 134, 739 (2013).
67. P. Lakshmi, K.S. Raj, and K. Ramachandran, *Cryst. Res. Technol.* 44, 153 (2009).
68. O. El-Tayeb, F. Mohammad, A. Hashem, and M. Aboulwafa, *Afr. J. Biotechnol.* 7, 4521 (2008).
69. S. Varavinit, N. Chaokasem, and S. Shobsngob, *Sci. Asia* 28, 247 (2002).

70. A.D. Saran, M.M. Sadawana, R. Srivastava, and J.R. Bellare, *Colloids Surf. A Physicochem. Eng. Asp.* 384, 393 (2011).
71. H. Dhyani, M.A. Ali, M.K. Pandey, B.D. Malhotra, and P. Sen, *J. Mater. Chem.* 22, 4970 (2012).
72. L.M. Hamilton, C.T. Kelly, and W.M. Fogarty, *Carbohydr. Res.* 314, 251 (1998).
73. F. Adnan, *Pak. J. Bot.* 42, 3507 (2010).
74. D. Gangadharan, K.M. Nampoothiri, S. Sivaramakrishnan, and A. Pandey, *Appl. Biochem. Biotechnol.* 158, 653 (2009).
75. N. Goyal, G. Sidhu, T. Chakrabarti, and J. Gupta, *World J. Microbiol. Biotechnol.* 11, 593 (1995).